IIETA International Information and Engineering Technology Association
Advancing the World of Information and Engineering

Revue des Composites et des Matériaux Avancés-Journal of Composite and Advanced Materials
Vol. 35, No. 2, April, 2025, pp. 253-265
Journal homepage: http://iieta.org/journals/rcma

Evaluation of the Infuence of Chemical Treatment of Olive Pomace Waste on the Thermophysical Properties of Aerated Concrete

Malika Atigui[1*], Youssef Maaloufa[1,2,3], Asma Souidi[1], Mina Amazal[1], Slimane Oubeddou[1], Hassan Demrati[1], Soumia Mounir[1,2,3], Ahmed Aharoune[1]

[1] Laboratory of Thermodynamics and Energetics, Faculty of Science, University of Ibn Zohr, Agadir 80000, Morocco
[2] National School of Architecture Agadir, New complex, University of Ibn Zohr, Agadir 80000, Morocco
[3] EMDD, CERNE2D, University Mohammed V, Rabat 20000, Morocco

Corresponding Author Email: malika.atigui@edu.uiz.ac.ma

https://doi.org/10.18280/rcma.350207

Received: 24 February 2025
Revised: 26 March 2025
Accepted: 11 April 2025
Available online: 30 April 2025

Keywords:
aerated concrete; durability; non-autoclaved; olive pomace; thermophysical properties; chemical treatment; thermal conductivity

ABSTRACT

In this study, we have decided to develop a composite material which is included in the list of building materials that would meet the requirements of thermal insulation while at the same time helping to protect the environment. To do this, we used waste from the olive oil extraction industry as a replacement for sand in non-autoclaved aerated concrete, we developed two types of mix, the first one by using olive pomace sand (OPU) with proportions of (0%, 10%, 20% ,30% and 40% by mass) and the other using the same proportions of olive pomace treated (OPT) with NaOH treatment, to study the effect of chemical treatment on the physical and thermal properties of this waste. The results obtained show that chemical treatment gives better physical properties and that this treatment improves thermal conductivity with gains of 0.64% and 2.93% for 30% and 40% respectively, and it is also found that it reduces the rate of water absorption and porosity for the 10% replacement percentage and shows a reduction rate of 31.2% and 23.5% respectively for untreated specimens and 34.4% and 24.5% for treated specimens.

1. INTRODUCTION

The energy consumption of most buildings, whether residential or industrial, is high if occupants are to be assured of acceptable thermal comfort. The implementation of energy-saving programmes in buildings should therefore be one of the priority actions. As part of the sustainable development, new regulations on thermal insulation in buildings are prompting scientists to seek out new materials for building energy-efficient systems that also ensure comfortable living environments.

It is a lightweight building material with exceptional technical properties such as adequate building resistance and outstanding thermal insulation. Aerated concrete is becoming more and more widely accepted as a building material for commercial and public buildings around the world [1]. Cellular concrete production techniques have been mastered for several decades, and the use of this type of concrete for building envelopes is commonplace. It is composed of a mixture of cement, sand, gypsum, lime, water and a blowing agent [2, 3]. Aerated concrete is manufactured by a process of hydrothermal synthesis of a binder of calcium silicate produced from a mixture of silica and lime [4]. When aluminium powder is added to the base mix, hydrogen is released. The bubbling is accompanied by the formation of C_3AH_6 hydrates produced by the reaction of lime with aluminium hydroxide, resulting in sufficient firming of the paste to stabilise the form of the expanded material [5]. In their current density range (400 to 800kg.m^{-3}), these types of material offer an reasonable compromise in terms of mechanical performance and thermal insulation [3].

The properties of aerated concrete have been improved by the use of many additives such as marble waste, rice husk ash, rice straw, polypropylene fibres, natural zeolite and bagasse ash [6-9], which improves the microstructure and, at the same time, the mechanical and thermal properties. Several researchers have used this waste as an additive [7-9], while others have used it to replace natural sand [4, 9-11].

Bhosale et al. [11] carried out a comparative study of the mechanical and physical properties of aerated concrete and clay, and found that the apparent density of aerated concrete is around 50% lower than that of clay. This is due to the porosity of aerated concrete, which reduces the permanent load on the masonry infill and construction costs. Cellular concrete also absorbs more water than clay.

Abhilasha et al. [12], in this study, the authors studied several types of additives used in aerated concrete, such as rice husks, natural zeolite and sugar sediments, etc. Based on the microstructure study of the composites, they noted that the presence of air voids in AAC gives it thermal insulation properties. Thanks to its thermal insulation properties, the energy consumption of buildings is reduced by around 50%. Fibre-reinforced aerated concrete has better thermophysical properties than AAC samples.

Zhang et al. [6], studied the effect of substituting silica fume and marble powder waste for cement on the mechanical properties and durability of aerated concrete. They found that increasing the rate of replacement by silica fume improves the mechanical properties of aerated concrete. With regard to the water absorption of aerated concrete, they have shown that the rate of absorption decreases significantly with the increase in the rate of cement replacement.

Pachla et al. [7], studied the effect of adding rice husk and rice straw on the properties of aerated concrete. They found that the addition of rice straw improved the thermal insulation of the composite.

Pehlivanlı and Uzun [9], stadied the effect of the length of polypropylene (PF) fibres on the thermal conductivity of autoclaved aerated concrete (AAC) was studied. They found that incorporating this type of fibre into aerated concrete resulted in an increase in thermal conductivity values. They also found that as the density of the AAC increased, the effect of the fibre on the thermal conductivity of the material also increased.

Karakurt et al. [13], used natural zeolite as an aggregate in the production of aerated concrete. They also found that the substitution of sand by zeolite sand decreases the weight of the aerated concrete specimens and increases the need for water, the thermal results obtained show that this material in general can be used as a thermal insulation material due to the values found in this study, the thermal conductivity varies from 0.08 up to 0.19$W.m^{-1}.k^{-1}$.

Zafar et al. [14], studied the use of granite dust as a partial replacement for sand in autoclaved aerated concrete, they observed an increase in density as the replacement rate increased, and a decrease in porosity and water absorption, for thermal conductivity, they noted an increase from 0.24 for the reference case to 0.33 for 20%.

Selvakumar et al. [10], studied the properties of aerated concrete with replacement of fine aggregate by foundry sand, they found that for the replacement of 20% foundry sand, the compressive strength increased and was considered the optimal replacement to improve strength. Analysis of the microstructure reveals isolated air voids, confirming the durability properties of aerated concrete.

From this literature review, it was concluded that aerated concrete has a lower density due to its porous structure, has a higher water absorption capacity so care needs to be taken when using it in external walls, and it is considered to be a thermal insulation material.

The aim of this study is to reduce the water absorption rate and improve the thermal properties by using olive pomace waste, we used this type of waste since it is more abundant in our region and its incorporation into aerated concrete reduces its environmental impact, and according to a literature review we found that this waste is not used with aerated concrete, and we treated our waste with the NaOH solution. This treatment is considered to be new work that has not been carried out before by other researchers, most researchers have used autoclaved aerated concrete with temperature and pressure conditions, we tried in our study to prepare non-autoclaved aerated concrete blocks to save energy. Therefore, in this study, we investigated the effect of partial substitution of natural sand by olive pomace waste on the performance of non-autoclaved aerated concrete, we treated this waste with NaOH solution to study the effect of chemical treatment on the properties of this waste, we used the following replacement rates: 0%, 10%, 20%, 30%, 40%. The thermal properties and microstructure of the prepared bricks, as well as the water absorption rate and porosity, were studied.

2. MATERIALS AND METHODS

2.1 Materials used

In this study, aerated concrete blocks were prepared by adding olive pomace waste as a partial substitute for sand. The following raw materials were used to prepare these blocks: CPJ 45 cement, natural sand, olive pomace sand, quicklime, gypsum, aluminium powder as an air-entraining agent and water. The olive pomace waste (Figure 1(a)) was recovered from a modern oil mill located in the Souss Massa region. They underwent a cleaning treatment with lukewarm water to separate the sediment of olive oil and the olive pulp (Figure 1(b)), after the washing step, this pomace was naturally dried in the open air for two days, then dried in an oven at 105°C for 24 hours (Figure 1(c)), and then crushed. The result of the grinding was sieved to obtain a sand grain size of between 0.08 and 2mm (Figure 1(d)). The olive pomace sand obtained was treated with NaOH solution to study the effect of treatment on the properties of this waste. The olive pomace sand is immersed in the solution at a concentration of 10% (by mass) for one hour at ambient temperature. It was then rinsed with distilled water to remove the excess of NaOH, after which it was dried in an oven at 70°C for 3 hours. This procedure is based on the work of Acharya et al. [15].

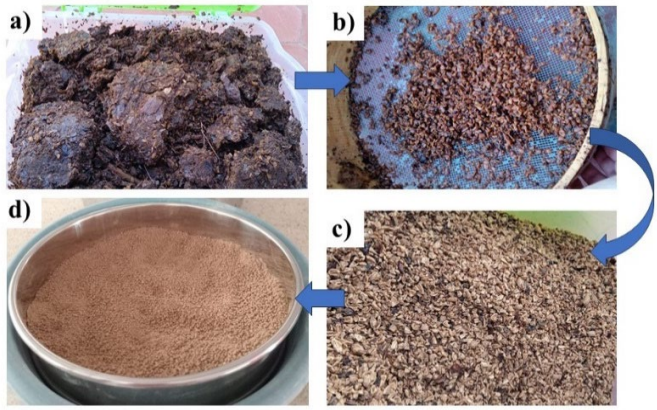

Figure 1. Waste preparation process

2.2 Specimens preparation

In the present work, two types of mixtures were prepared, one replacing natural sand with untreated olive pomace sand (OPU) and the other with olive pomace treated with sodium hydroxide solution (OPT) in order to determine the effect of treatment on the properties of this waste. After a literature study on the replacement percentages used, we chose five percentages (0%, 10%, 20%, 30% and 40%) to study the effect of replacing natural sand with olive pomace sand and at the same time to reduce the environmental impact by recycling this waste. Two types of masonry were prepared manually under laboratory conditions: specimens with dimensions of $4\times4\times16cm^3$ (Figure 2 (a)) for the mechanical and capillary water absorption tests, and others with dimensions of $10\times10\times2.5cm^3$ for the thermal tests (Figure 2 (b)), we prepared sex specimens for each percentage for the specimens dedicated

to the mechanical test and the water absorption test and two specimens for the ones dedicated to the thermal tests. During the formation of the aerated concrete blocks, they began to expand and swell under the effect of the bubbles formed from the reaction of the aluminium powder in the past, the prepared blocks were air-dried for 24 hours and demoulded, after this, they had been stored under laboratory conditions for 28 days. The types of composites prepared and the physical quantities of the constituents of each mixture are shown in Table 1.

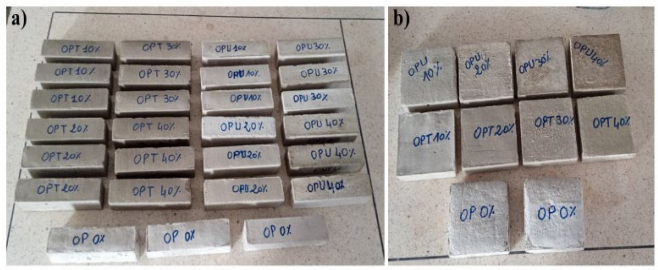

Figure 2. The specimens elaborated

Table 1. Materials used in the production of composites

Sample	Cement (g)	Sand (g)	Lime (g)	Gypsum (g)	Olive Pomace (g)	Aluminium Powder (g)	W/B
OP	100	325	75	5	0	1.1	0.65
OPU10	100	292.5	75	5	32.5	1.1	0.65
OPU20	100	260	75	5	65	1.1	0.65
OPU30	100	227.5	75	5	97.5	1.1	0.65
OPU40	100	195	75	5	130	1.1	0.65
OPT10	100	292.5	75	5	32.5	1.1	0.65
OPT20	100	260	75	5	65	1.1	0.65
OPT30	100	227.5	75	5	97.5	1.1	0.65
OPT40	100	195	75	5	130	1.1	0.65

W/B ratio set after several tests with W: Water et B: Binder
B = cement + lime + gypsum

2.3 The physical and chemical attributes of materials

Table 2 displays the results of the physical and chemical analysis for olive pomace waste before and after treatment. A reduction in both water content and water absorption is observed following the treatment, with a reduction rate of 25.59% and 14.24% respectively, so it can be said that the olive pomace sand absorbs a greater quantity of water, which may affect the mechanical behavior of the concrete [16, 17] while the treated olive pomace sand has a lower water absorption rate than the untreated olive pomace sand. It can be concluded that the treatment of the waste with sodium hydroxide solution leads to a reduction in the water absorption rate. The loss on ignition is calculated by the variation in weight of a specimen after it has been heated to a high temperature (1000°C) in accordance with the norm NBN EN 15169, which has caused the combustion or volatilisation of part of its contents. We see a very high value for the untreated specimen but this value decreases for the treated specimen. The same results found in the case of the organic matter content, so the treatment of waste with NaOH reduces the organic matter content of this waste. We calculated the organic matter content using the Walkley and Black method [18], which is used to determine organic carbon and is calculated using the following relationship Eq. (1).

$$\% MO = \% C \times 1.724 \quad (1)$$

We have also measured the pH, electrical conductivity and salinity of the two types of OP sand using a pH meter (Figure 3) which can measure both pH and electrical conductivity. The study of waste salinity is more important as it affects the mechanical behaviour of the compounds and can cause corrosion problems [19]. Soil is considered to be saline if the electrical conductivity is greater than 4000µS.cm^{-1} [20]. In our study, we find that the salinity of the waste increases when treated with NaOH but presents an acceptable value of 1.3 ppT and the electrical conductivity presents a value of 2530µS.cm^{-1}. So, this waste is not saline, the pH value shows that olive waste is acidic, but after treatment the pH value increases and becomes basic.

Table 2. Chemical properties of untreated and treated OP

Parameter	OP Untreated	OP Treated
Water content (%)	4.26	3.17
Loss on ignition (%)	90.92	87.08
water absorption (%)	92.7	79.5
pH	5.61	8.09
Electrical conductivity (µS.cm^{-1})	1243.3	2530
Salinity (ppT)	0.62	1.3
Organic carbon content (%)	27.31	24.69
Organic matter content (%)	47.08	42.56

The development of a composite requires a perfect knowledge of the granulometry since the resistance of the concrete depends essentially on the aggregate. Figure 4 shows the particle size curves for the two types of sand, olive pomace and natural sand, which makes it possible to distinguish between aggregates according to the granular classes specified in standard NF EN 933-1. From the grading curve we calculated the fineness modulus, Curvature coefficient (Cc) and Uniformity coefficient (Cu) which are presented in Table 3. The fineness modulus is an important characteristic, a good concrete sand must have a fineness modulus not exceeding 3.2. Natural sand contains finer elements than olive pomace sand since the fineness modulus value of olive pomace sand is higher than that of natural sand. For Uniformity coefficient, we find that the two types of sands are superior to 3. Therefore, the granulometry is varied or spread out [21]. The Curvature coefficient for natural sand is 1.29 and for olive pomace sand is 1.38. The grading curve then descends fairly evenly, indicating the presence of a wide variety of diameters (1<Cc<3) [21]. From the sand equivalence value, we can see that it exceeds 80%, so we can say that both types of sands are very clean. The specific surface area of sand indicates its real surface area as opposed to its apparent surface area. It corresponds to the total surface area per unit of mass and is

expressed in m²/g. In our case, we calculated the value of the specific surface area of the two sands using the methylene blue method. The specific surface area of natural sand is 5.86m².g^{-1} whereas that of olive pomace sand is 2.93m².g^{-1}, implying that olive pomace sand has larger particle sizes than natural sand.

Table 3. The physical and particle size properties of natural and olive pomace sand

Parameter	Norm	Unite	Naturel Sand	Olive Pomace
Real density	NF EN1097-6	g.cm^{-3}	0.72	1.21
Apparent density	NF EN1097-6	g.cm^{-3}	1.31	2.41
Porosity Intergranular	NF P18459	%	45.04	49.79
Fineness modulus	NF-P18-540		1.38	2.9
Cu	--		4.38	5.43
Cc	--		1.29	1.38
VBS	NF-P94-068		0.28	0.14
SST	NF-P94-068	m².g^{-1}	5.86	2.93
E.S.V	NM-10.1.147		96.28	94.48
E.S	NM-10.1.147		84.54	85.03

Cu: Uniformity coefficient, Cc: Curvature coefficient, VBS: Soil blue value, SST: Total specific surface area, E.S.V: Visual sand equivalence, E.S: Sand equivalence

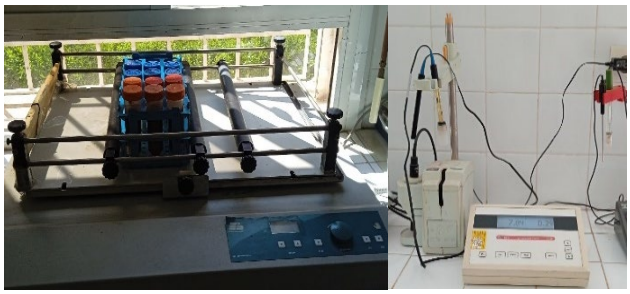

Figure 3. pH and electrical conductivity measuring instruments

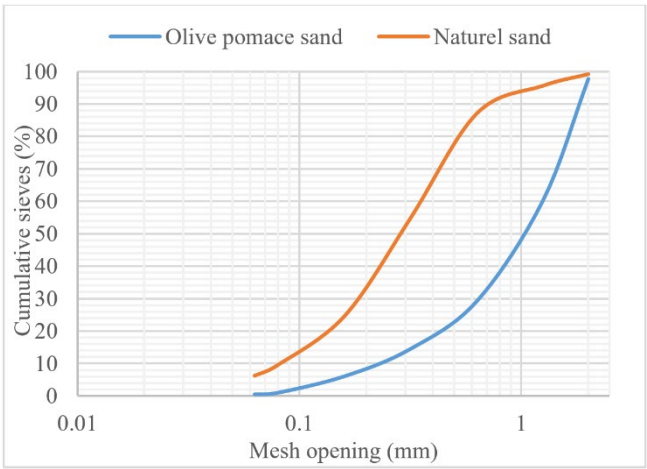

Figure 4. Particle size curves for the two types of sand

Figure 5 shows the morphology of the OP sand before and after treatment. We see that the OP sand has a different distribution of sizes and a non-smooth surface; it also shows the existence of virgin fibres with multiple pores and cavities, and numerous small materials, filaments and other impurities can be found on the surface of the untreated particles (Figure 5 (a)). It has been observed in Figure 5 (b) that the sodium hydroxide solution can significantly clean the surface of the grains and eliminate the small filaments. We can also see that the surface of the grains becomes rough after the treatment, this modification is in fact due to the elimination of lignin and hemicellulose, this observation is reported by other authors [22, 23]. This modification of the surface of the treated grains can have positive effects on the composite, it can improve adhesion between the matrix and the additive as the surface becomes rougher, and it can modify the porous structure of the grains which can reduce the water absorption capacity, this structure can also improve thermal conductivity [24]. Figure 6 shows the microstructure of natural sand (Figure 6(a)) compared with that of olive pomace sand (Figure 6(b)). We can see that the two types of sand represent different particle sizes, with olive pomace sand having larger particles than natural sand, which corresponds to the results of the VBS test (Table 3). By analysing the chemical composition of the two different types of sand using energy dispersive X-ray spectroscopy (EDS) (Figure 7), we can see that OP sand contains carbon and oxygen with mass percentages of 42.83% and 57.17% respectively, while natural sand contains several chemical elements such as oxygen with a percentage roughly equal to that of OP sand in addition to silicon, iron and aluminium.

Figure 8 shows the DRX image of olive pomace waste before and after treatment using the Bruker D8 Advance Twin diffractometer. The phases identified before treatment are quartz with a proportion of 24%, magnesium dihydrogen phosphate and pyrazole with proportions of 30% and 36% respectively; these phases were identified by other researchers [25-27], but after treatment the aluminium phosphate phase appears with a proportions of 25% and the magnesium dihydrogen phosphate rate decreases to 30%. The crystallinity of olive pomace waste in relation to the calcination level is shown in Figure 9. It can be seen that before calcination this waste contains quartz, pyrazole and magnesium dihydrogen, but after calcination at a temperature of 200°C, small peaks of calcite appear, due to the decomposition of calcium carbonate, which is present in this waste in a negligible percentage, for calcination at 400°C, magnesium dihydrogen phosphate and pyrazole completely disappear and calcite appears (64%), sodalite and dolomite also appear , which is due to the decomposition of magnesium and pyrazole under the effect of temperature, we also see the disappearance of sodalite and that dolomite decomposes at 800°C to the formation of calcium hydroxide.

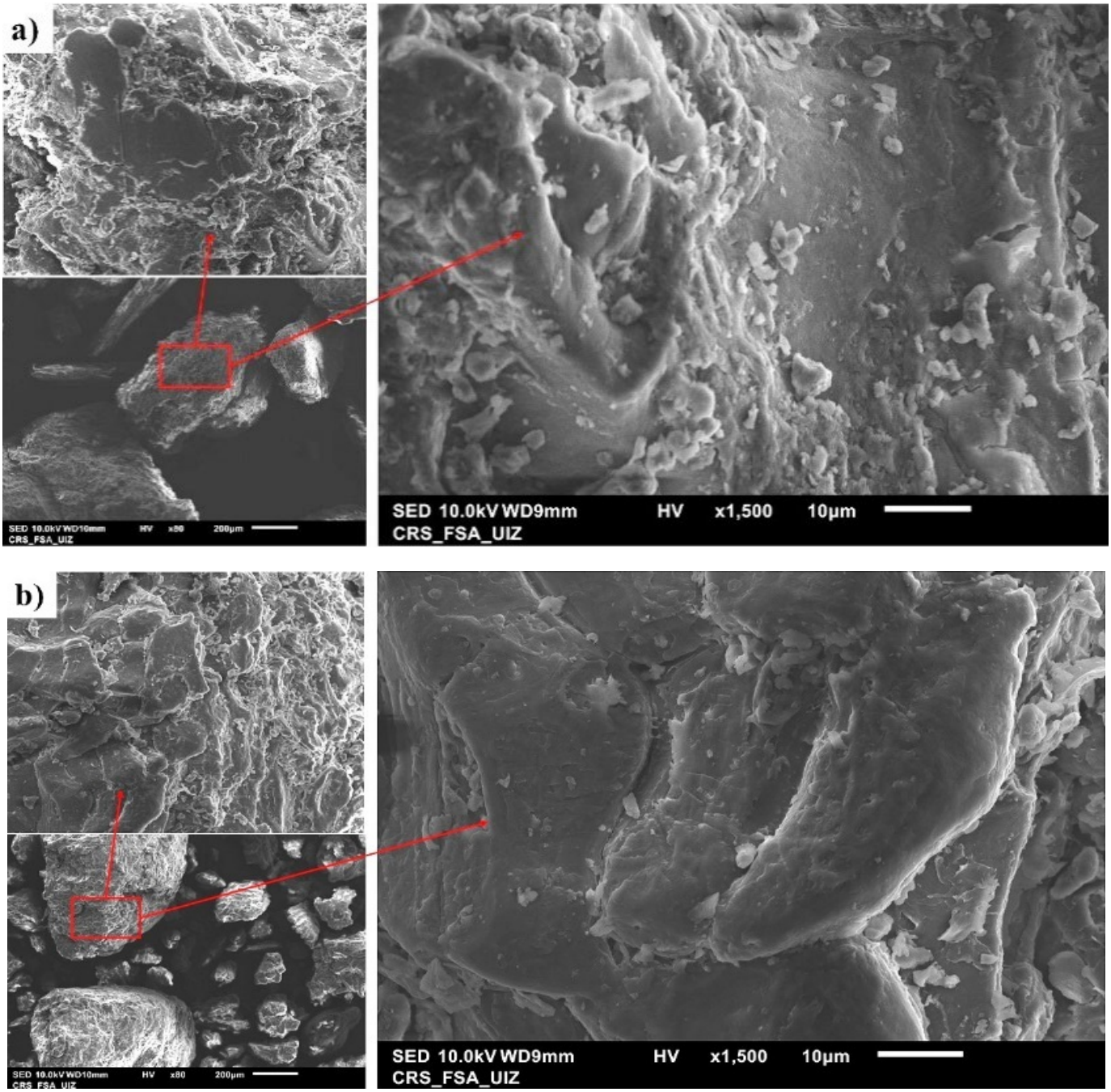

Figure 5. SEM observation of olive pomace sand (a) untreated (b) treated

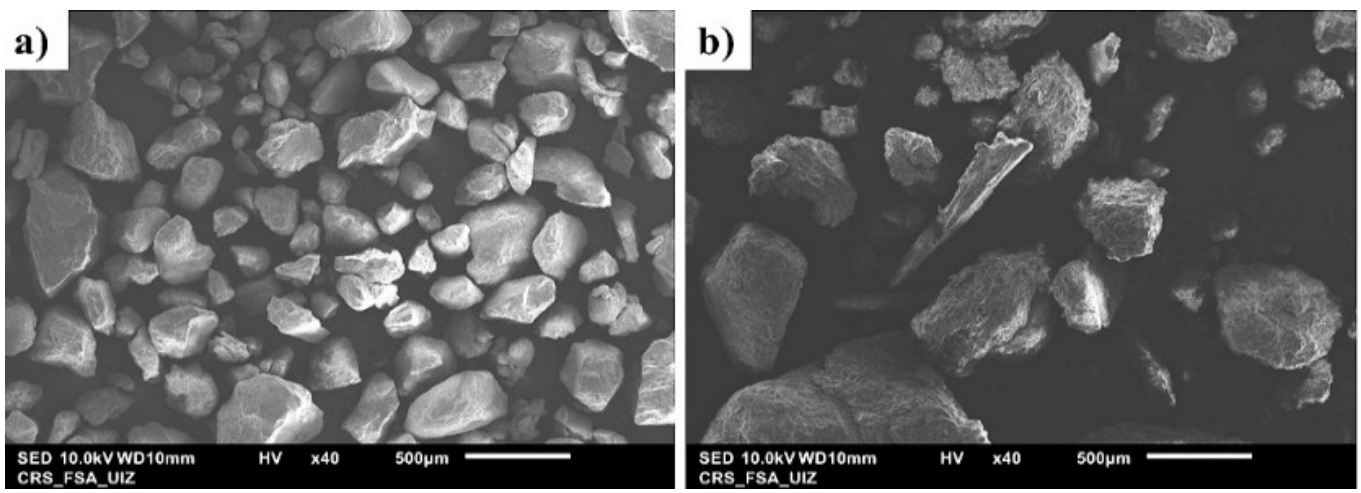

Figure 6. SEM observation of (a) natural sand and (b) olive pomace sand

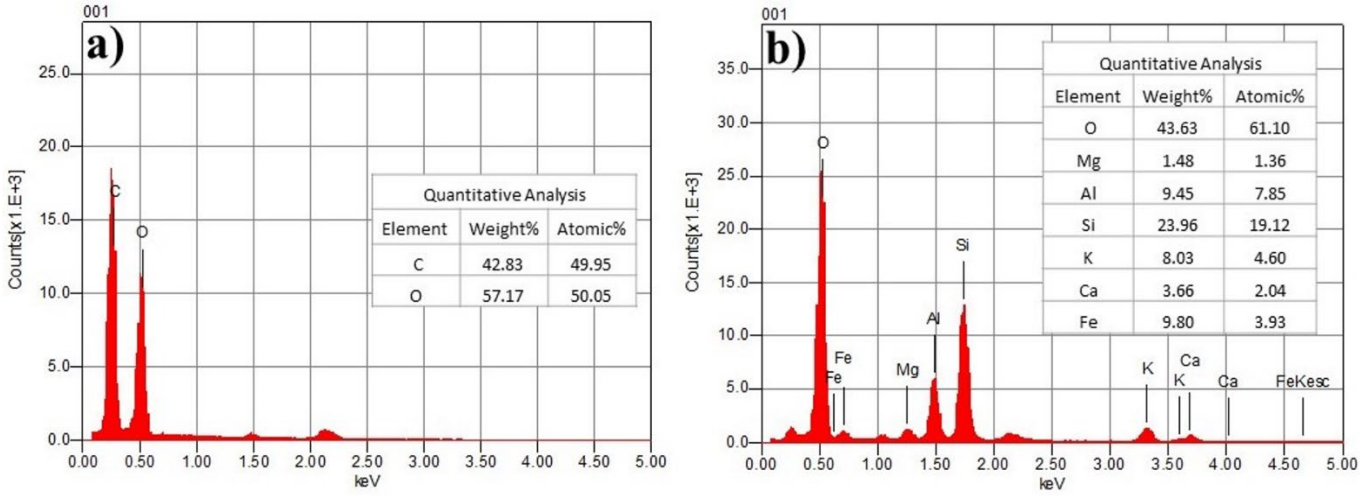

Figure 7. Chemical composition of the (a) OP sand and (b) natural sand

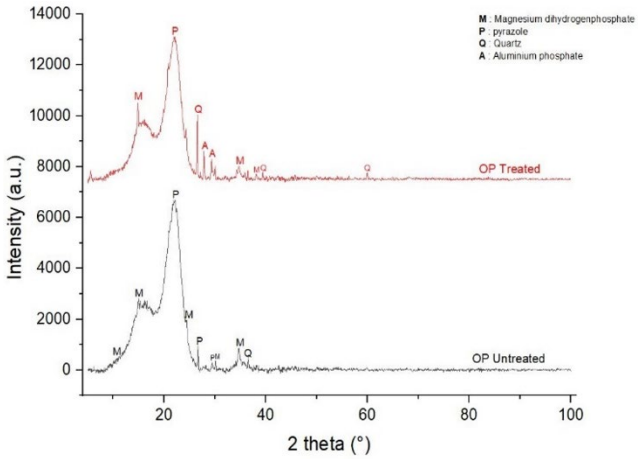

Figure 8. Diffractogram of OP untreated and treated

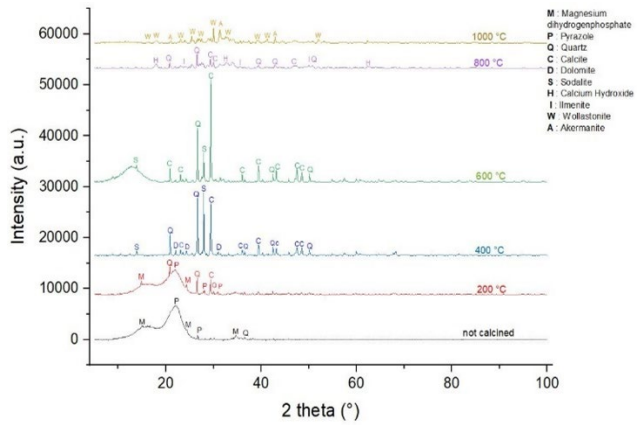

Figure 9. The crystalline nature of OP waste vs the calcination degree

2.4 Test methods

2.4.1 Scanning electron microscope (SEM) analysis

A scanning electron microscope (SEM) was employed to study the morphologies of the OPU and OPT raw materials and the surface of the composites produced. The device used is a JEOL JSM IT-100 (Figure 10), coupled to an EDXS (Energy Dispersive X-Rays Spectroscopy) X-ray emission detector, which makes it possible to measure the local quantitative composition of a specimen. The sample surface was gold coated in order to get clear SEM images.

Figure 10. Scanning electron microscope equipment

2.4.2 Dry density, wet density

In this study, dry density, wet density of the samples were tested in accordance with standard NF EN 772-13. For the dry density tests, specimens measuring 10×10×2.5cm^3 after 28 days of curing in open air were placed in an oven at 70°C until the mass stabilised. These specimens were considered completely dry.

2.4.3 Water absorption and accessible porosity

The water absorption and the porosity accessible to water are calculated according to Eqs. (2) and (4) respectively. This method makes it possible to calculate pore volume.

Absorption after immersion (%):

$$\frac{M_2 - M_1}{M_1} \times 100 \quad (2)$$

Absorption after immersion and boiling (%):

$$\frac{M_3 - M_1}{M_1} \times 100 \quad (3)$$

Volume of permeable pore space (porosity) (%):

$$\frac{M_3 - M_1}{M_3 - M_4} \times 100 \quad (4)$$

where, M_1 is the dry mass, M_2 is the mass of the sample in air after immersion, M_3 is the mass of the sample in air after immersion and boiling, M_4 is the mass of the sample in water after immersion and boiling.

2.4.4 Thermal conductivity

The HOT DISK TPS 1500 transient plane source (TPS) method allows the characterisation of the thermal properties of various materials in a matter of minutes. It is increasingly being used for the evaluation of the thermal conductivity of insulation materials, especially in the construction industry. In our study, the thermal test samples ($10\times10\times2.5cm^3$) are oven-dried at 70°C until they stabilise, after measuring their thermal conductivity, as shown in Figure 11.

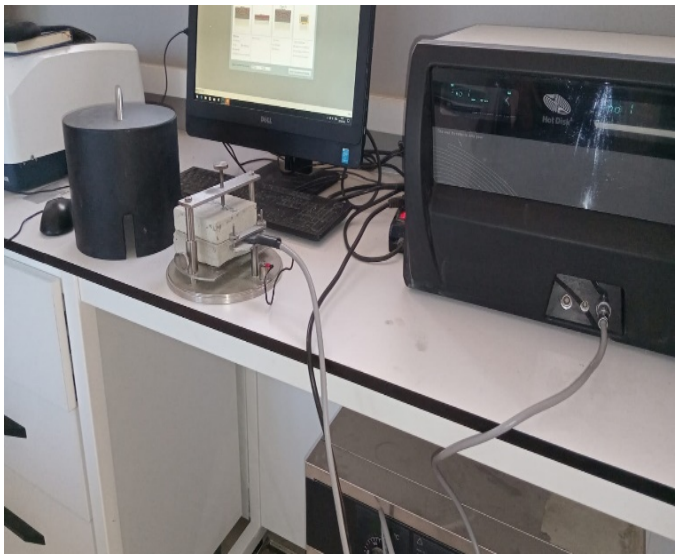

Figure 11. Thermal properties measurement

3. RESULTS AND DISCUSSION

3.1 Microstructure

Figure 12 displays the morphology of non-autoclaved aerated concrete, we can clearly see the presence of numerous minuscule cells with micropores and macropores, the macropores are clearly visible in black, with diameters of the order of 535µm and 240µm.

During the preparation of the past, we observed that the incorporation of olive sand reduced the swelling of the paste and consequently air bubbles, which justified the microstructure results. The SEM images in Figure 13 show that the incorporation of olive-pomace sand into aerated concrete increases the solid matrix and decreases the pore diameter (Figure 13 (a) and Figure 13 (b)). The diameter then becomes of the order of 106µm and 56µm for OPU20 and OPU40 respectively, which is due to the filling of the pores by the olive pomace grains. An improvement in the distribution of the pores in the matrix is also observed, the same observation is reported by other authors [15, 28]. For the treated composites, Figures 13 (c) and 13 (d) show the microstructure of OPT20 and OPT40 respectively. It can be seen that they have a more homogeneous surface with fewer pores than the reference, but there is an increase in pore diameter compared with the untreated composites. A better dispersion of the olive pomace particles in the matrix is also observed. This dispersion is due to the rugosity of the olive pomace particles, which results in better adhesion of the OPT particles to the matrix as shown in Figure 14. This means that the treatment enhances the compatibilities between the olive pomace grains and the matrix, other researchers have treated other types of waste with this solution and found results similar to ours [29]. It has been found that treating olive pomace with the hydroxide solution improves adhesion between the olive pomace and the matrix by removing natural and artificial impurities that have accumulated on the olive pomace surface.

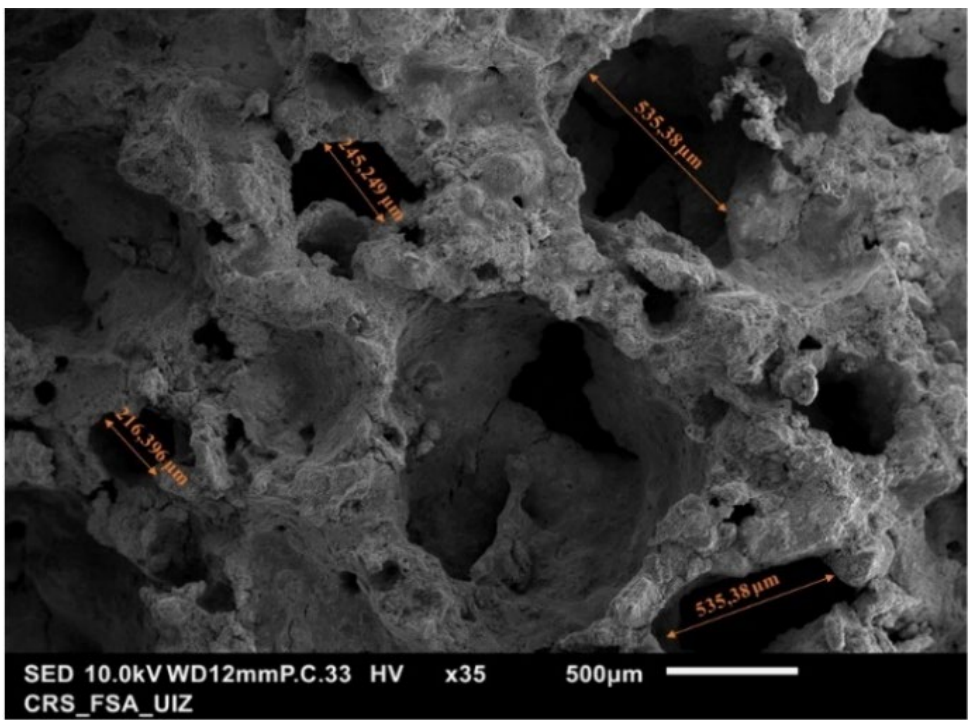

Figure 12. Morphological representation of the reference specimen OP0

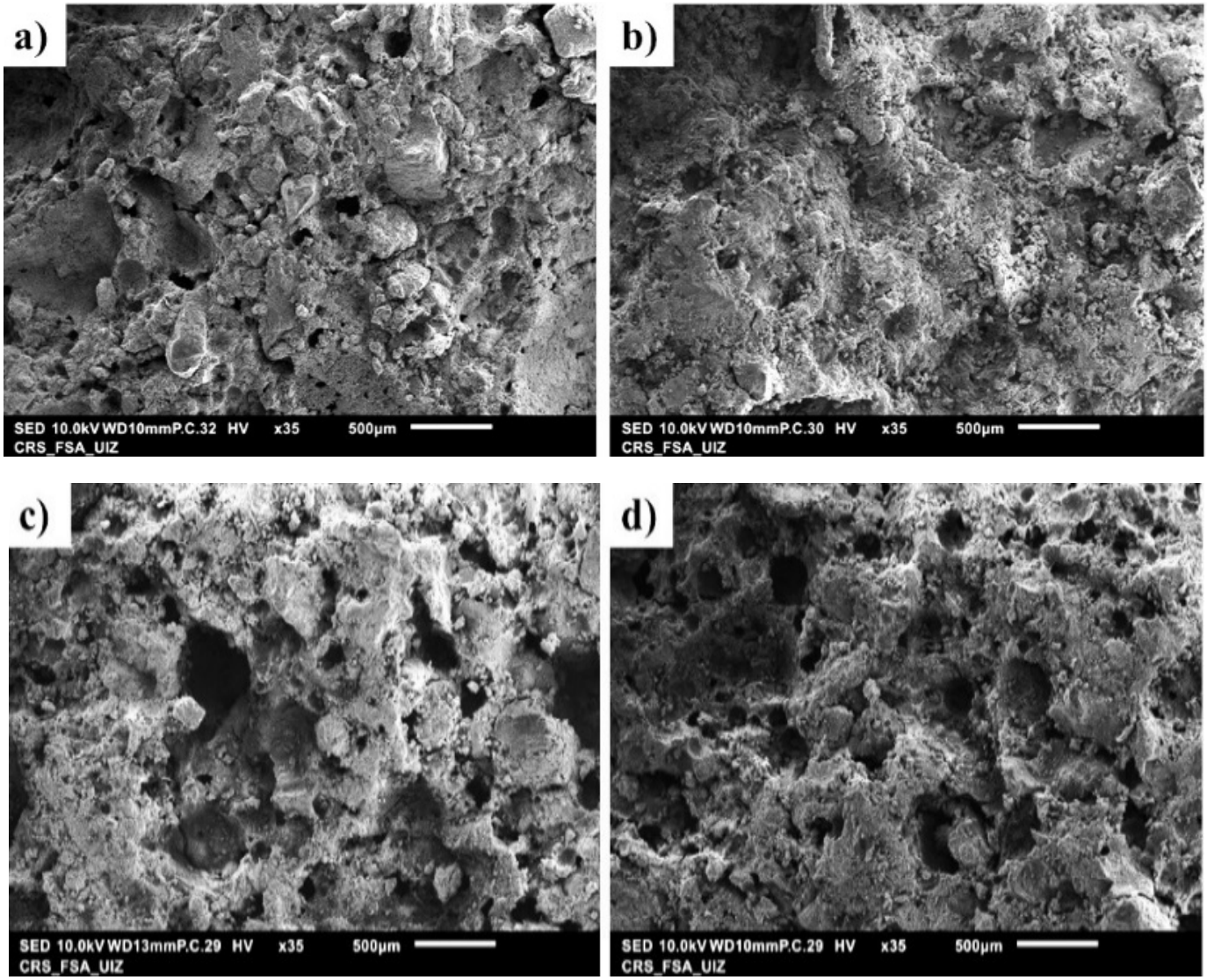

Figure 13. Morphological representation of composites (a) OPU20 (b) OPU40 (c) OPT20 (d) OPT40

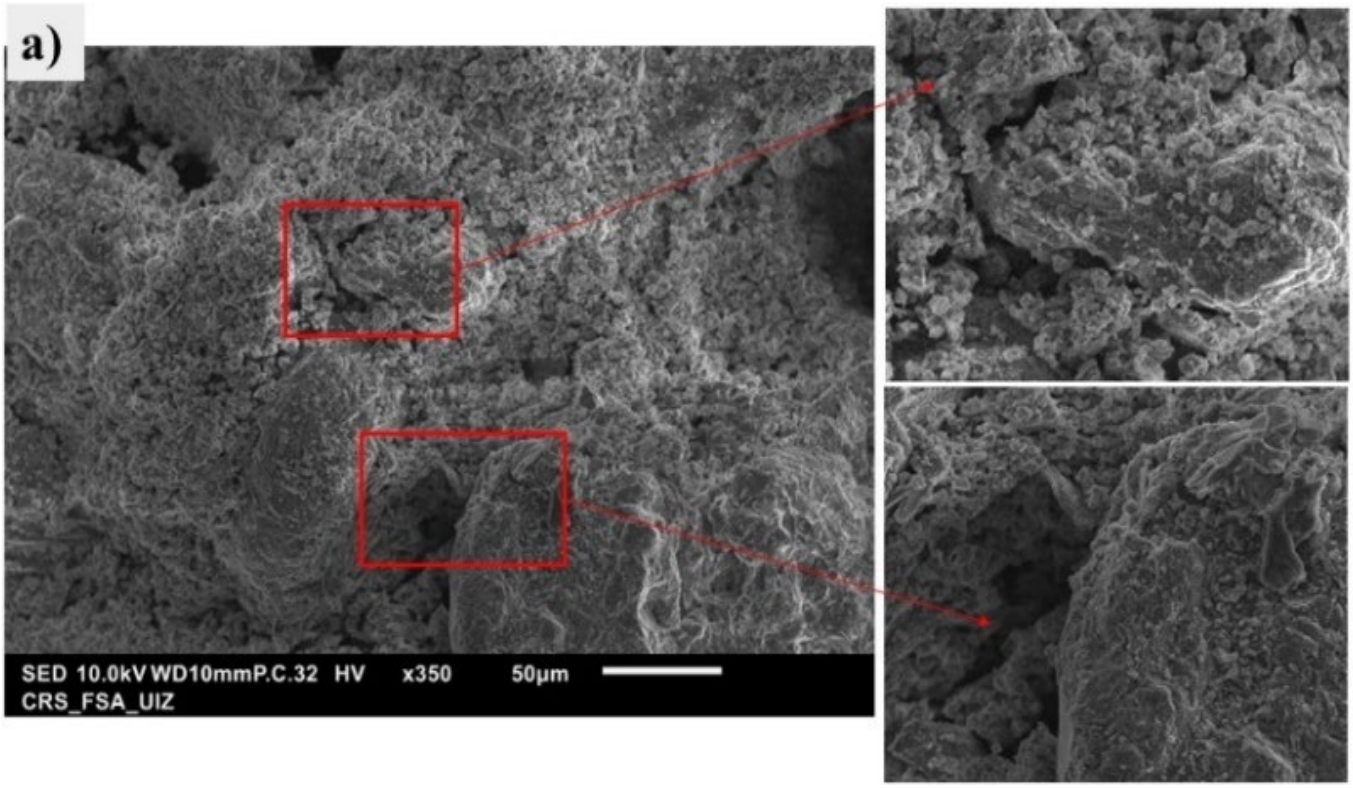

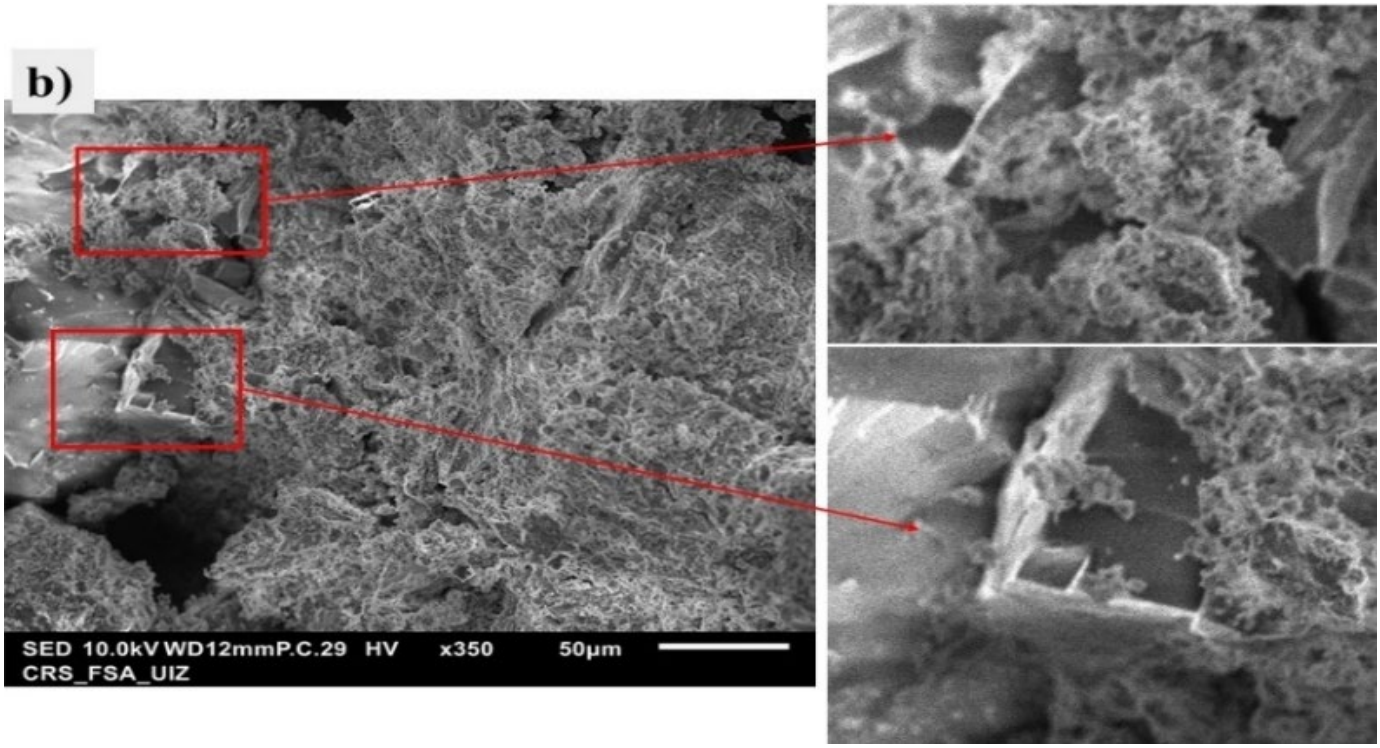

Figure 14. SEM visualizations of the composites (a) OPU20 (b) OPT20

3.2 Dry and wet density

The quality of aerated concrete depends on its dry density, according to standard NF P 12-024-2 the dry density of pure aerated concrete varies between 350 and 850kg.m^{-3}, in our case we found that the dry density of OP0 is 780kg.m^{-3} in accordance with the norm, but the replacement of natural sand by olive pomace sand increases the density for both treated and untreated cases as illustrated in Figures 15 (a) and 15 (b). the dry density varies between 780 and 1120kg.m^{-3} for the case of untreated OP substitution, and between 780 and 1170kg.m^{-3} for the case of NaOH treatment, these results are consistent with those of other researchers [15, 30]. The wet density showed the same evolution as the dry density, with the 10% replacement rate showing the maximum value, 1183kg.m^{-3} and 1184kg.m^{-3} for the composites before and after treatment respectively with a percentage increase of almost 0.52 for both cases. Figure 16 shows the relationship between the dry and wet densities. It can be seen that there is a correlation between these two quantities, and this correlation is indicated by other researchers [31, 32].

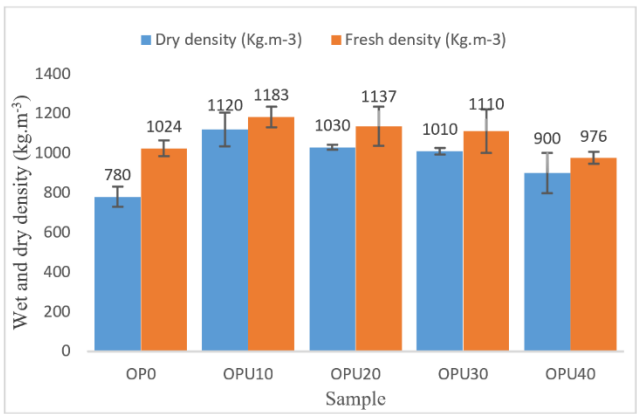

(a)

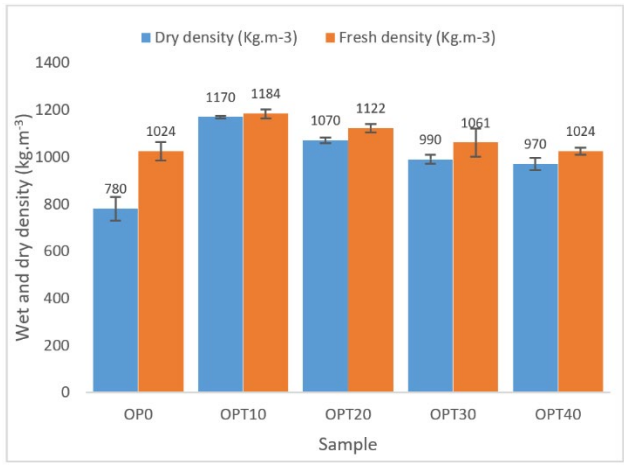

(b)

Figure 15. (a) Dry and wet density of untreated composites, (b) Dry and wet density of treated composites

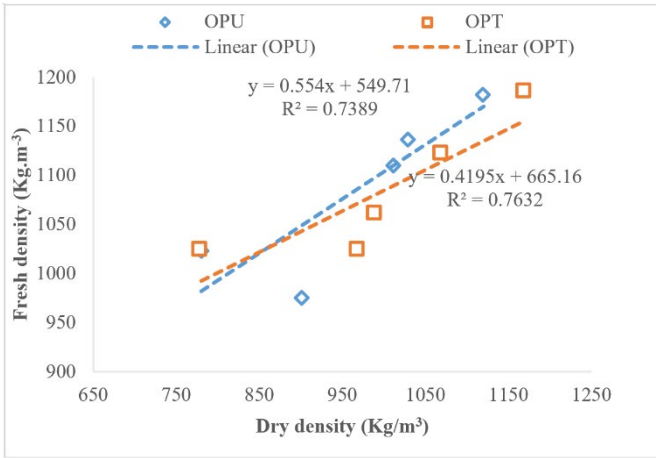

Figure 16. The relationship between dry and wet density

3.3 Water absorption and accessible porosity

In general, the water absorption coefficient depends on pore size and pore distribution. Porous concrete can absorb a lot of water, unlike normal concrete. As we have seen in the microstructure of aerated concrete (Figure 12), aerated concrete contains macropores and micropores, so porosity is the sum of macropores and micropores, which confirms the results obtained in Table 4, the water absorption and porosity of pure cellular concrete take on values of 37.34% and 48.83% respectively, but the incorporation of olive pomace decreases these two values for the 10% percentage with a decrease rate of 31.2% and 23.5% respectively for untreated specimens and 34.4% and 24.5% for treated specimens. but these values start to increase with the percentage increase and reach a maximum value for the 40% substitution rate of treated olive pomace sand but do not exceed the reference value as illustrated in Figures 17 and 18. Figure 19 shows the evolution of porosity as a function of water absorption. It can be seen that there is a good correlation between these two quantities, and that the increase in the rate of replacement of natural sand by olive pomace sand leads to an increase in water absorption and composite porosity.

Table 4. Absorption of water and porosity of the samples

Sample	Water Absorption (%)	Porosity (%)
OP0	37.34	48.83
OPU10	25.69	36.23
OPU20	26.33	37.77
OPU30	26.95	38.27
OPU40	28.85	39.94
OPT10	24.49	36.87
OPT20	27.24	38.57
OPT30	31.92	41.83
OPT40	34.79	43.13

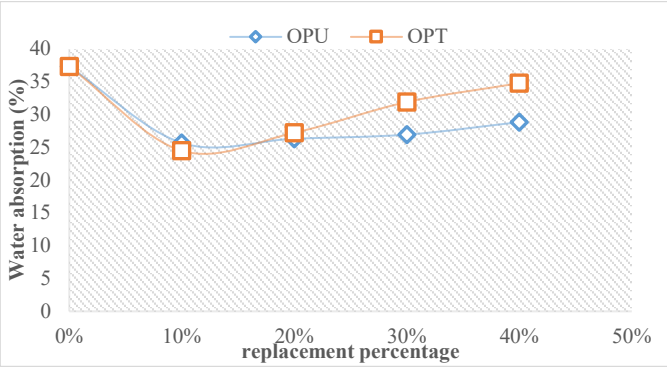

Figure 17. Water absorption as a function of replacement rates

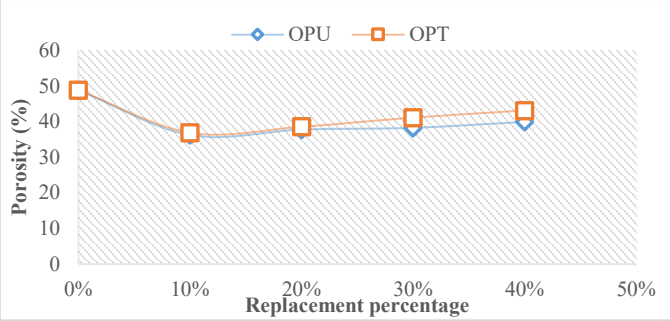

Figure 18. The porosity as a function of replacement rates

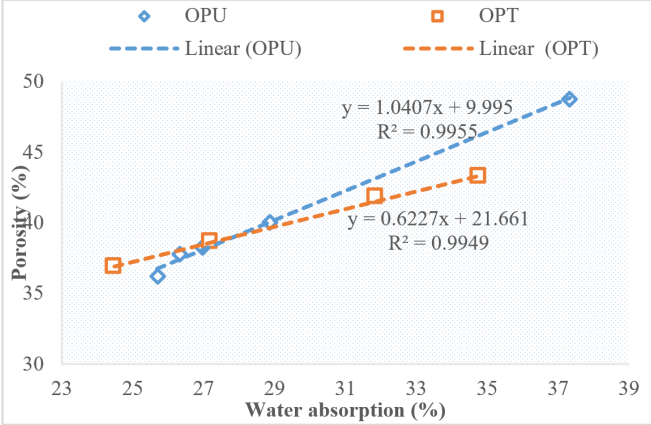

Figure 19. Relation between water absorption and porosity

3.4 Thermal properties

Thermal conductivity and diffusivity of composites are shown in Table 5. Consistent with the microstructural results, it can be seen that the incorporation of olive pomace grains into aerated concrete blocks increase the thermal conductivity due to the reduction in pore size. This observation is also cited by other researchers [10], other researchers have also found that thermal conductivity increases as the percentage of additive increases [9], but in our case it increases and then starts to decrease. Figure 20 shows the variation of thermal conductivity as a function of the rate of replacement of natural sand by OP sand, an increase in thermal conductivity was observed for the 10% replacement rate, but it starts to decrease as the substitution rates increase, and presents better results for the 40% substitution rate for the treated composites.

Comparing treated and untreated composites, we can see that treating the grains with the soda solution gives better results, with gains of 0.64% and 2.93% for 30% and 40% respectively, while the 40% percentage gives results close to those of the reference. It can therefore be said that chemical treatment improves thermal conductivity by increasing the porosity and surface roughness of the treated grains, as shown in the microstructure of the composites (Figure 13). A linear correlation can be observed between dry density and thermal conductivity, as shown in Figure 21.

Figure 22 shows the correlation between thermal conductivity and composite porosity. A linear correlation is observed between these two parameters, with thermal conductivity decreasing as porosity increases.

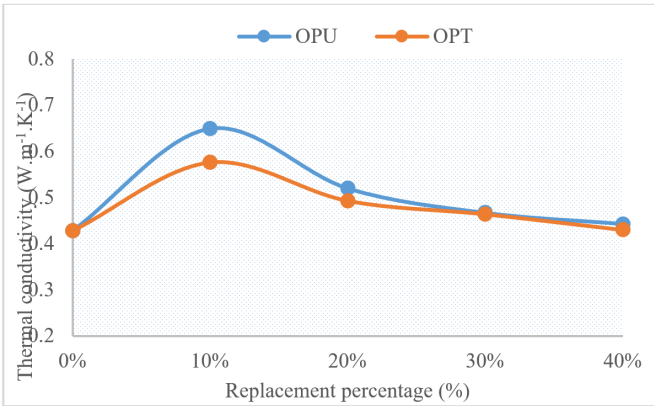

Figure 20. Thermal conductivity as a function of replacement rate

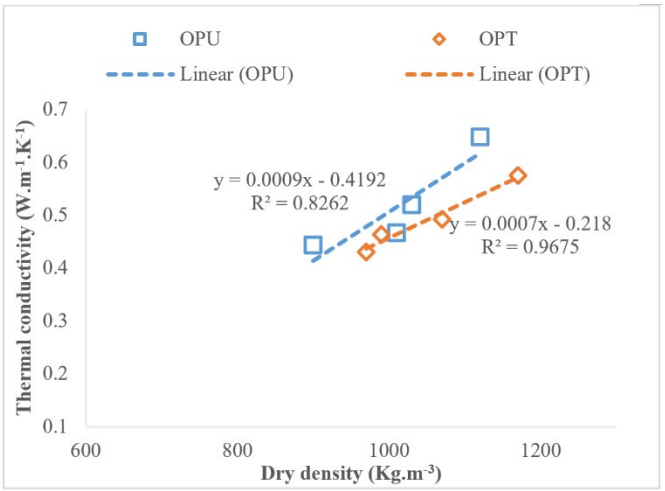

Figure 21. Thermal conductivity vs dry density of composites

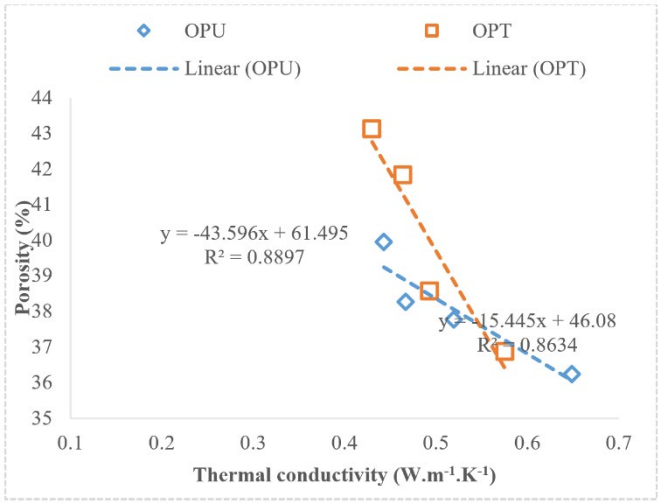

Figure 22. Thermal conductivity vs composite porosity

Table 5. Thermal behavior of the different composites elaborated

	Thermal Conductivity ($W.m^{-1}.K^{-1}$)					Thermal Diffusivity ($mm^2.s^{-1}$)				
	λ_1	λ_2	λ_3	λ_{ave}	$\Delta\lambda/\lambda$ (%)	α_1	α_2	α_3	α_{ave}	$\Delta\alpha/\alpha$ (%)
OP0	0.419	0.425	0.44	0.428	2.803	0.325	0.354	0.376	0.35	6.919
OPU10	0.637	0.65	0.662	0.649	1.898	0.355	0.363	0.366	0.361	1.291
OPU20	0.509	0.524	0.529	0.520	1.600	0.352	0.369	0.379	0.366	3.363
OPU30	0.459	0.469	0.474	0.467	1.426	0.294	0.309	0.316	0.306	3.155
OPU40	0.442	0.445	0.444	0.443	0.300	0.299	0.305	0.317	0.307	3.257
OPT10	0.567	0.571	0.591	0.576	2.544	0.341	0.36	0.38	0.360	5.457
OPT20	0.492	0.488	0.5	0.493	1.351	0.353	0.357	0.371	0.360	2.960
OPT30	0.465	0.463	0.464	0.464	0.215	0.498	0.505	0.506	0.503	0.596
OPT40	0.425	0.428	0.438	0.430	1.781	0.291	0.3	0.324	0.305	6.229

4. CONCLUSION

This study examines the potential of utilizing waste from the olive oil extraction industry as a partial replacement for sand in non-autoclaved aerated concrete. Using this waste offers several advantages, such as reducing the volume of waste sent to landfills and minimizing its impact on both human health and the environment. This waste was incorporated into the aerated concrete matrix in proportions ranging from 0% to 40% with a step size of 10%. This study focuses mainly on the chemical modification of the surface of the olive pomace grains and the effect of treating this waste with NaOH on the thermophysical properties of the specimens. We have developed two types of blocks, one using the waste without treatment and the other with treatment by the sodium hydroxide solution. The conclusions of this study are as follow:

1) Chemical treatment of olive pomace particles with NaOH produces stiffer materials and improves the adhesion between the olive pomace and the matrix by removing natural and artificial impurities that have accumulated on the surface of the OP grains.
2) The incorporation of olive pomace waste increases the density of the blocks compared with the reference. This is due to the reduction of air bubbles during the preparation of the paste and the reduction of pores, but the density of the composites containing the waste decreases with the increase in the rate of replacement for the case of treated and untreated blocks, the maximum density was observed in the specimens treated with NaOH.
3) The water absorption and porosity of pure aerated concrete are 37.34% and 48.83% respectively, but the incorporation of olive pomace reduces both these values.
4) The addition of olive grains to aerated concrete blocks increases thermal conductivity for OPU10 due to the reduction in pore size but this value starts to improve with the addition of this waste and the chemical treatment improves thermal conductivity when increasing the substitution rate more than 10%, this is because porosity increases in the case of treated composites, and alkaline treatment improves adhesion between the matrix and the additive, which in turn improves thermal conductivity.

All of this work has highlighted the beneficial effects of treating olive pomace to improve roughness and adhesion between the grains and the matrix, reduce water absorption, improve thermal conductivity of aerated concrete.

ACKNOWLEDGMENTS

The authors wish to express their sincere gratitude to the Research Centre of the Faculty of Sciences of Agadir, Ibn Zohr University, for their support. They would also like to extend their thanks to the technicians at the Public Laboratory for Tests and Studies (LPEE) for their assistance with the mechanical aspects of the work.

REFERENCES

[1] Peng, Y., Liu, Y., Zhan, B., Xu, G. (2021). Preparation of autoclaved aerated concrete by using graphite tailings as an alternative silica source. Construction and Building Materials, 267: 121792. https://doi.org/10.1016/j.conbuildmat.2020.121792

[2] Cai, L., Li, X., Ma, B., Lv, Y. (2018). Effect of binding materials on carbide slag based high utilization solid-wastes autoclaved aerated concrete (HUS-AAC): Slurry, physic-Mechanical property and hydration products. Construction and Building Materials, 188: 221-236. https://doi.org/10.1016/j.conbuildmat.2018.08.115

[3] Chen, C., Liu, X., Wang, X., Jiu, S., Chen, Y., Liu, Y. (2025). Development of sustainable non-autoclaved aerated concrete: Influence of aluminium powder on mechanical properties and pore structure of geopolymers based on rockwool furnace bottom slag waste. Construction and Building Materials, 472: 140957. https://doi.org/10.1016/j.conbuildmat.2025.140957

[4] Jiang, J., Lu, X., Niu, T., Hu, Y., Wu, J., Cui, W., Zhao, D., Ye, Z. (2022). Performance optimization and hydration characteristics of BOF slag-Based autoclaved aerated concrete (AAC). Cement and Concrete Composites, 134: 104734. https://doi.org/10.1016/j.cemconcomp.2022.104734

[5] Shan, C., Yang, Z., Su, Z., Rajan, R., Zhou, X., Wang, L. (2022). Preparation and characterization of waterproof autoclaved aerated concrete using molybdenum tailings as the raw materials. Journal of Building Engineering, 49: 104036. https://doi.org/10.1016/j.jobe.2022.104036

[6] Zhang, S., Cao, K., Wang, C., Wang, X., Wang, J., Sun, B. (2020). Effect of silica fume and waste marble powder on the mechanical and durability properties of cellular concrete. Construction and Building Materials, 241: 117980. https://doi.org/10.1016/j.conbuildmat.2019.117980

[7] Pachla, E.C., Silva, D.B., Stein, K.J., Marangon, E., Chong, W. (2021). Sustainable application of rice husk and rice straw in cellular concrete composites. Construction and Building Materials, 283: 122770. https://doi.org/10.1016/j.conbuildmat.2021.122770

[8] Kunchariyakun, K., Asavapisit, S., Sinyoung, S. (2018). Influence of partial sand replacement by black rice husk ash and bagasse ash on properties of autoclaved aerated concrete under different temperatures and times. Construction and Building Materials, 173: 220-227. https://doi.org/10.1016/j.conbuildmat.2018.04.043

[9] Pehlivanlı, Z.O., Uzun, I. (2022). Effect of polypropylene fiber length on mechanical and thermal properties of autoclaved aerated concrete. Construction and Building Materials, 322: 126506. https://doi.org/10.1016/j.conbuildmat.2022.126506

[10] Selvakumar, M., Geetha, S., Lakshmi, S.M. (2022). Investigation on properties of aerated concrete with foundry sand as replacement for fine aggregate. Materials Today: Proceedings, 65: 1666-1673. https://doi.org/10.1016/j.matpr.2022.04.709

[11] Bhosale, A., Zade, N.P., Sarkar, P., Davis, R. (2020). Mechanical and physical properties of cellular lightweight concrete block masonry. Construction and Building Materials, 248: 118621. https://doi.org/10.1016/j.conbuildmat.2020.118621

[12] Abhilasha, Kumar, R., Lakhani, R., Mishra, R.K., Khan, S. (2023). Utilization of solid waste in the production of autoclaved aerated concrete and their effects on its physio-Mechanical and microstructural properties: Alternative sources, characterization, and performance insights. International Journal of Concrete Structures and Materials, 17(1): 6. https://doi.org/10.1186/s40069-022-00569-x

[13] Karakurt, C., Kurama, H., Topcu, I.B. (2010). Utilization of natural zeolite in aerated concrete production. Cement and Concrete Composites, 32(1): 1-8. https://doi.org/10.1016/j.cemconcomp.2009.10.002

[14] Zafar, M.S., Javed, U., Khushnood, R.A., Nawaz, A., Zafar, T. (2020). Sustainable incorporation of waste granite dust as partial replacement of sand in autoclave aerated concrete. Construction and Building Materials, 250: 118878. https://doi.org/10.1016/j.conbuildmat.2020.118878

[15] Acharya, P., Pai, D., Mahesha, G.T. (2023). Effect of chemical treatments on physical and mechanical characteristics of Helicteres isora natural fiber. Materials Today: Proceedings. https://doi.org/10.1016/j.matpr.2023.03.432

[16] Ge, W., Wang, A., Zhang, Z., Ge, Y., Chen, Y., Li, W., Jiang, H., Shuai, H., Sun, C., Yao, S., Qiu, L. (2023). Study on the workability, mechanical property and water absorption of reactive powder concrete. Case Studies in Construction Materials, 18: e01777. https://doi.org/10.1016/j.cscm.2022.e01777

[17] de Oliveira Morais, P.A., de Souza, D.M., Madari, B.E., da Silva Soares, A., de Oliveira, A.E. (2019). Using image analysis to estimate the soil organic carbon content. Microchemical Journal, 147: 775-781. https://doi.org/10.1016/j.microc.2019.03.070

[18] Long, Z., Zhang, R., Wang, Q., Xie, C., Zhang, J., Duan, Y. (2022). Mechanism analysis of strength evolution of concrete structure in saline soil area based on 15-year service. Construction and Building Materials, 332: 127281. https://doi.org/10.1016/j.conbuildmat.2022.127281

[19] Souidi, A., Maaloufa, Y., Amazal, M., Atigui, M., Oubeddou, S., Mounir, S., Idoum, A., Aharoune, A. (2024). The effect of mussel shell powder on the thermal and mechanical properties of plaster. Construction and Building Materials, 416: 135142. https://doi.org/10.1016/j.conbuildmat.2024.135142

[20] Thior, M., Sané, T., Sy, O., Descroix, L., Ndiaye, L.G., Sambou, A.K., Cissokho, D., Solly, B. (2019). Caractéristiques granulométrique et dynamique sédimentaire entre les différentes unités géomorphologiques du littoral de la Casamance, Sénégal. La Revue Ivoirienne des Sciences et Technologie, 33: 189-213.

[21] Fagerlund, G. (1973). Determination of specific surface by the BET method. Matériaux et Construction, 6: 239-245. https://doi.org/10.1007/BF02479039

[22] Izwan, S.M., Sapuan, S.M., Zuhri, M.Y.M., Mohamed, A.R. (2020). Effects of benzoyl treatment on NaOH treated sugar palm fiber: Tensile, thermal, and morphological properties. Journal of Materials Research and Technology, 9(3): 5805-5814. https://doi.org/10.1016/j.jmrt.2020.03.105

[23] Poletanovic, B., Janotka, I., Janek, M., Bacuvcik, M., Merta, I. (2021). Influence of the NaOH-Treated hemp

fibres on the properties of fly-Ash based alkali-activated mortars prior and after wet/dry cycles. Construction and Building Materials, 309: 125072. https://doi.org/10.1016/j.conbuildmat.2021.125072
[24] Dinesh, S., Elanchezhian, C., Devaraju, A., Sivalingam, S.K., Velmurugan, V. (2021). Comparative study of mechanical and morphological analysis of NaOH treated and untreated banana fiber reinforced with epoxy hybrid composite. Materials Today: Proceedings, 39: 861-867. https://doi.org/10.1016/j.matpr.2020.10.652
[25] de la Casa, J.A., Castro, E. (2014). Recycling of washed olive pomace ash for fired clay brick manufacturing. Construction and Building Materials, 61: 320-326. https://doi.org/10.1016/j.conbuildmat.2014.03.026
[26] Harrami, M., El Fami, N., Moussadik, A., Khachani, N., Taibi, M., Diouri, A. (2022). Elaboration and characterization of composite clays based on "Coal waste-Olive pomace" mixtures. Materials Today: Proceedings, 58: 1573-1577. https://doi.org/10.1016/j.matpr.2022.03.555
[27] Atigui, M., Maaloufa, Y., Souidi, A., Amazal, M., Oubeddou, S., Demrati, H., Mounir, S., Aharoune, A. (2024). Enhanced thermo-Physical properties of gypsum composites using olive pomace waste reinforcement. Journal of Composite & Advanced Materials/Revue des Composites et des Matériaux Avancés, 34(1): 67-75. https://doi.org/10.18280/RCMA.340109.
[28] Al-Shwaiter, A., Awang, H. (2023). Effect of elevated temperatures on strength and microstructural characteristics of foam concrete containing palm oil fuel ash as sand replacement. Construction and Building Materials, 376: 131052. https://doi.org/10.1016/j.conbuildmat.2023.131052
[29] Assaggaf, R.A., Maslehuddin, M., Al-Dulaijan, S.U., Al-Osta, M.A., Ali, M.R., Shameem, M. (2022). Cost-Effective treatment of crumb rubber to improve the properties of crumb-Rubber concrete. Case Studies in Construction Materials, 16: e00881. https://doi.org/10.1016/j.cscm.2022.e00881
[30] Ahmad, M.R., Pan, Y., Chen, B. (2021). Physical and mechanical properties of sustainable vegetal concrete exposed to extreme weather conditions. Construction and Building Materials, 287: 123024. https://doi.org/10.1016/j.conbuildmat.2021.123024
[31] Souza, T.B., Lima, V.M., Araújo, F.W., Miranda, L.F., Neto, A.A.M. (2021). Alkali-Activated slag cellular concrete with expanded polystyrene (EPS)-physical, mechanical, and mineralogical properties. Journal of Building Engineering, 44: 103387. https://doi.org/10.1016/j.jobe.2021.103387
[32] Amazal, M., Mounir, S., Souidi, A., Atigui, M., Oubeddou, S., Maaloufa, Y., Aharoune, A. (2024). Production and characterization of a composite based on plaster and juncus maritimus plant fibers. Fluid Dynamics & Materials Processing, 20(9). https://doi.org/10.32604/FDMP.2024.050613

NOMENCLATURE

OPU	Olive pomace untreated
OPT	Olive pomace treated
SEM	Scanning electron microscope
EDS	Energy-dispersive X-ray spectroscopy
XRD	X-Ray diffraction analysis

Greek symbols

α	Thermal diffusivity, $m^2. s^{-1}$
λ	Thermal conductivity, $W.m^{-1}.K^{-1}$

Subscripts

Cu	Uniformity coefficient
Cc	Curvature coefficient
VBS	Soil blue value
SST	Total specific surface
E.S.V	Visual sand equivalence
E.S	Sand equivalence